Received: 27 June 2024 | Revised: 30 August 2024 | Accepted: 18 September 2024

DOI: 10.1002/mp.17448

TECHNICAL NOTE

MEDICAL PHYSICS

Design, construction, and use of a tapered-spiral, quadrature $^{1}H/^{23}Na$ double-tuned coil for *in ovo* MRI at 7 T

Chang-Hoon Choi[1,2] | **Suk-Min Hong**[1] | **Jörg Felder**[1,3] | **Maximilian Bruch**[1,2] | **Wieland A. Worthoff**[1] | **Sandra Krause**[1] | **N. Jon Shah**[1,4,5,6]

[1]Institute of Neuroscience and Medicine – 4, Forschungszentrum Jülich, Juelich, Germany

[2]Aachen University of Applied Sciences, Jülich, Germany

[3]RWTH University, Aachen, Germany

[4]Institute of Neuroscience and Medicine – 11, Forschungszentrum Jülich, Juelich, Germany

[5]JARA – BRAIN – Translational Medicine, Aachen, Germany

[6]Department of Neurology, RWTH Aachen University, Aachen, Germany

Correspondence
Chang-Hoon Choi, Institute of Neuroscience and Medicine – 4, Forschungszentrum Jülich, Jülich 52425, Germany.
Email: c.choi@fz-juelich.de

Abstract

Background: *In ovo* MR presents a promising and viable alternative to traditional in vivo small animal experiments. Sodium MRI complements proton MRI by providing potential access to tissue cellular metabolism. Despite its abundance, sodium MRI is challenged by lower MR sensitivity and faster relaxation times compared to proton MRI. Ensuring a high signal-to-noise ratio and effective B_0 shimming is essential. Double-tuned coils combining ^{23}Na and ^{1}H are frequently employed to achieve structural imaging and efficient shim adjustment.
Purpose: This study introduces a novel, highly optimized, double-tuned coil design, specifically for MR scans of chick embryos.
Methods: A tapered-spiral, double-tuned coil was designed and constructed following careful consideration of design parameters. The performance of the coil was rigorously assessed through bench tests, and final validation was conducted on a 7 T MRI scanner using a chick embryo.
Results: Bench tests demonstrated that the return losses for both ^{1}H and ^{23}Na coils were better than – 30 dB, and isolation factors were better than – 21 dB, indicating that the double-tuned coil was well-set, with negligible coupling between channels. MR images of chick embryos, obtained using the coil, validated the feasibility of utilizing the design concept for *in ovo* applications.
Conclusions: The innovative design of the proposed double-tuned coil, characterized by its unique arrangement, offers improved performance. This design has the potential to significantly enhance the quality of *in ovo* ^{1}H and ^{23}Na measurements.

KEYWORDS
chick embryo, double-tuned coil, dual-tuned coil, *in ovo*, MRI, sodium, X-nuclei

1 | INTRODUCTION

Non-proton MRI studies are currently of great interest due to their ability to provide valuable cellular and metabolic information.[1,2] Sodium (^{23}Na) MRI, for example, complements proton MRI by offering insights into the critical sodium-potassium exchange across cell membranes and the characteristics of cell metabolism.[3] Tissue sodium concentration can reveal substantial information regarding various pathologies.[4–7] Although ^{23}Na is the second most abundant MR-sensitive element in living organisms, and despite the signal-to-noise ratio (SNR) enhancements afforded by ultra-high field MRI systems and advanced MR technologies, ^{23}Na MRI remains challenging. This is due to sodium's inherently lower MR sensitivity and much faster relaxation times compared to protons.[8] Therefore, maintaining a high SNR for the sodium signal is crucial. Additionally, static magnetic field (B_0) shimming with the low ^{23}Na signal is problematic. Consequently, the simultaneous or

subsequent acquisition of proton imaging is advantageous. In this context, double-tuned coils, comprising both a ^{23}Na coil and a ^{1}H coil, are frequently employed.[9] This arrangement provides high-resolution anatomical images and enables effective B_0 shimming capability.

The utilization of double-tuned coils mitigates the issue of sample re-positioning encountered with separate RF coils in sequential acquisition scans. However, it can also result in several degrees of signal or functionality loss in the X-nuclei coil, dependent on the double-tuned coil design. Conventionally, double-tuned birdcage coils have been the preferred coil design and have been adapted in various configurations for different applications. These include alternating rungs,[10] transformer-coupled,[11] spiral/twisted,[12,13] and four-ring[14] arrangements, as well as designs incorporating traps[15,16] or PIN-diodes.[17] A critical challenge for these designs is addressing the coupling between coils resonating at two or more distinct frequencies. Minimizing this coupling is a crucial factor in determining the quality of a double-tuned coil.

The traditional birdcage coil designs, such as alternating rungs, traps, and PIN-diodes, introduce lossy components that degrade image quality, particularly on the X-nuclear channel.[15–18] In contrast, spiral and four-ring birdcage coil designs do not include these components, but they necessitate structural modifications to the coil, which may degrade its quality and adaptability. For instance, the four-ring design requires an optimized inner and outer rung length ratio, which generally results in a substantial increase in overall coil length. This additional length requirement for the outer end-rings limits the accessible space, which can be problematic.[19] Several innovative approaches[20–26] have been explored to maintain the quality of the non-proton coil, ensuring that it remains comparable to its single-tuned equivalent while also maintaining the quality of the images delivered by the proton coil.

This current work introduces a novel, highly optimized, double-tuned coil design specifically dedicated to MR scans of chick embryos. The use of chick embryos as an alternative to traditional animal models has garnered increasing attention. Chick embryos offer simplicity in screening and preparation protocols, coupled with several distinct advantages, such as convenient access to their chorioallantoic membranes (CAMs) shared phylogenetic traits with mammals, rapid growth rates, and cost-effectiveness.[27,28] The primary evaluation metrics of the coil performance were rigorously assessed on the bench, and final validation was performed on a 7 T MRI scanner using a chick embryo.

2 | MATERIALS AND METHODS

Given the aforementioned factors, the following criteria were considered when designing the double-tuned coil for ^{1}H/^{23}Na *in ovo* applications: (1) optimize the ^{23}Na performance to match the quality of the coil as high as its single-tuned coil, and ideally surpassing the standard birdcage coil, while minimizing coupling between ^{1}H and ^{23}Na without introducing any lossy components; (2) ensure that the structure of both the ^{1}H and ^{23}Na coils provides identical field-of-view (FOV) coverage; and (3) maintain high-quality ^{1}H imaging.

Figure 1 presents our proposed design, showing both a photograph of the assembled coil and circuit diagrams of the individual ^{1}H and ^{23}Na coils. As the chick embryo moves randomly within the eggshell,[29] a birdcage coil design that covers the entire embryo volume was selected to mitigate the uncertainty of the position of the embryo's head. In terms of the ^{23}Na coil design, we incorporated a tapered structure (towards the end-rings) into a standard birdcage coil, enhancing efficiency throughout the egg and improving the SNR, particularly near the end-rings,[29] while achieving extended coverage. Moreover, this design has the potential to decrease coupling near the end-rings between the ^{1}H and ^{23}Na coils, likely due to the increased separation distance. For integrating the ^{1}H coil with the ^{23}Na coil, we initially employed a geometrically isolated design approach, that is, with the rungs of the ^{1}H coil rotated by 22.5[30,31] in the axial domain relative to the rungs of the ^{23}Na coil. However, the coupling between the ^{1}H and ^{23}Na frequencies was still too substantial, considerably degrading the ^{1}H image quality and resulting in artefacts. Therefore, a spiral winding pattern was implemented for the ^{1}H coil,[12,13] with an angle of approximately 50° from the end-rings. This spiral design further benefits in the SNR and coverage towards the end-rings along the z-axis.[12,32]

After careful consideration of the design parameters, we designed and constructed a tapered-spiral, double-tuned coil. The ^{1}H coil, tuned to 297.2 MHz corresponding to our 7 T system, operates in a high-pass configuration, and the ^{23}Na coil, tuned to 78.6 MHz, functions with a low-pass configuration. Both coils were driven in quadrature mode to enhance performance. The coil formers were meticulously designed using 3D CAD software (Inventor, Autodesk, California, USA) and manufactured on an in-house 3D printer (Fortus 400mc, Stratasys, Minnesota, USA) using the biocompatible polycarbonate material. This approach enabled us to incorporate curved features while also precisely replicating thin yet robust coil cases, which are essential for maintaining coil sensitivity by minimizing sensitivity loss due to filling factor discrepancies. Our modified birdcage coil maintains the same dimensions (70 mm in length, 50 mm in diameter) as previously employed but integrates the aforementioned curved feature for enhanced performance. Copper tapes were utilized as conductors for both the ^{23}Na coil (6 mm width) and the ^{1}H coil end-ring patterns (4 mm width), while 1 mm silver-coated copper wire was chosen for the ^{1}H coil rungs due to its flexibility and ease of handling, ensuring a set distance from the ^{23}Na coil.

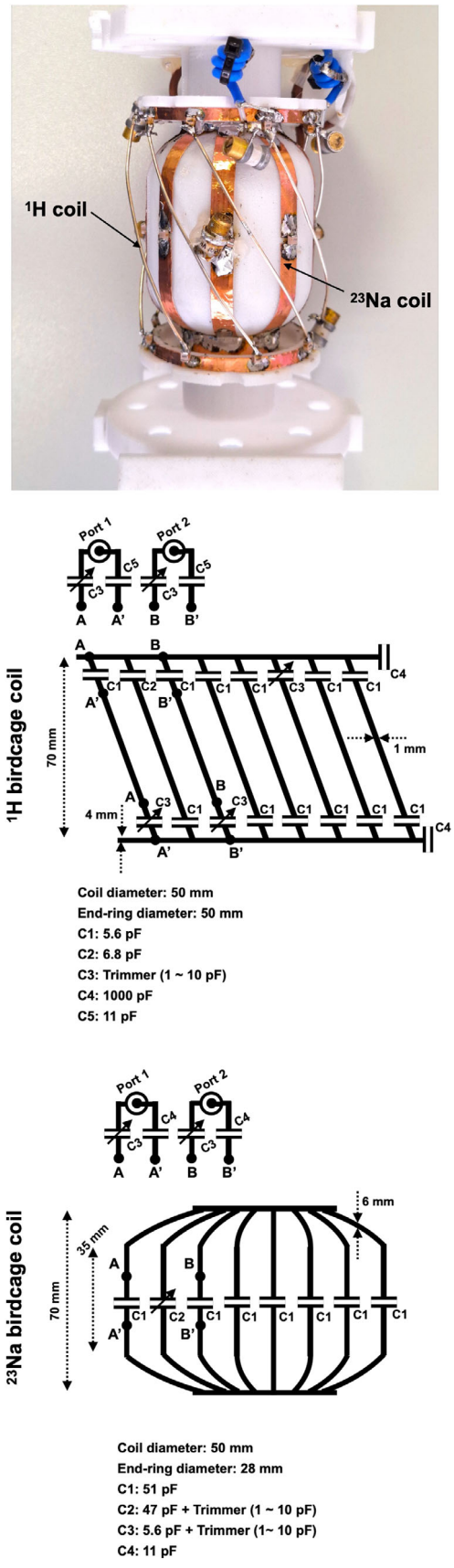

FIGURE 1 A photograph of the complete coil and circuit diagrams of the ^{1}H and ^{23}Na coils featuring detailed dimensions and component values.

The tuning of the ^{1}H / ^{23}Na coil was achieved using 5.6 pF/51 pF non-magnetic fixed capacitors (100B, Delicap, China), respectively, with each point on the matching network (A, A', B and B') directly connected to corresponding points (A, A', B and B') on the coils. Fine adjustments to their frequencies, decoupling between channels, and the attainment of a 50Ω matching condition were facilitated via non-magnetic trimmers (1–10 pF). Having loaded the chick embryo, the return losses (S_{11} and S_{22}) and the isolation (S_{21}) of these coils were comprehensively measured using a vector network analyzer (ZNB4, Rohde & Schwarz, Germany) on the bench. Coaxial-cable-wound cable traps tuned to each nucleus were built and integrated into each channel of the double-tuned coils.

One pathogen-free fertilized chick embryo (Valo BioMedia GmbH, Germany) suitable for medical purposes was selected for *in ovo* measurements on embryo developmental day 13. The egg was subsequently incubated at a temperature of 37.8°C with a humidity level of 54% in a benchtop incubator (HEKA Favorit-Olymp 192, Germany). In order to mitigate image degradation due to excessive movement of the embryo during the MR measurements, the chick embryo was anesthetized by pipetting a calculated amount of liquid isoflurane onto a piece of tissue paper to reach 2% isoflurane within the coil former.

The MR measurement was conducted on a 7 T Terra MRI scanner (Siemens Healthineers, Erlangen, Germany) with specific parameters: for ^{1}H imaging (sequence = T_2-weighted Turbo Spin Echo, resolution = 0.35 × 0.35 mm^2, FOV = 78 × 78 mm^2, matrix size = 224 × 224, slice thickness = 0.7 mm, repetition time (TR) = 5120 ms, echo time (TE) = 50 ms, averages = 8, acquisition time (TA) = 7:25 min) and for ^{23}Na imaging (sequence = 3D FLASH, resolution = 1 × 1 × 1 mm^3, FOV = 180 × 180 mm^2, matrix size = 180 × 180, TR = 20 ms, TE = 4.2 ms, averages = 32, TA = 15:49 min, pixel bandwidth = 120 Hz). Co-registration of the ^{1}H and ^{23}Na images was facilitated using ITK-SNAP software.[33]

3 | RESULTS

The bench test results of the coils' responses are presented in Table 1. The scattering (S)-parameters, the S_{11} and S_{33} for ^{1}H and the S_{22} and S_{44} for ^{23}Na coils were better than – 30 dB. Additionally, the S_{31} and S_{42} of both coils were better than – 21 dB. This indicates that both coils were well-tuned and -matched, with negligible coupling between channels in the individual ^{1}H and ^{23}Na coils. Furthermore, the coupling values between the ^{1}H and ^{23}Na coils (S_{21}, S_{23}, S_{41} and S_{43}) at the ^{1}H and ^{23}Na frequencies were better than – 18 dB and – 24 dB, respectively, further demonstrating outstanding isolation between the quadrature channels of

TABLE 1 Scattering (S)-parameters (reflection loss, isolation between two channels) of the proposed double-tuned $^{1}H/^{23}Na$ coil.

S-parameters	^{1}H FREQUENCY	^{23}Na frequency
S_{11}	N/A	– 37.2 dB
S_{22}	– 31.2 dB	N/A
S_{33}	N/A	– 54.2 dB
S_{44}	– 37.5 dB	N/A
S_{31}	N/A	– 21.5 dB
S_{42}	– 21.1 dB	N/A
S_{21}	– 18.5 dB	– 25.8 dB
S_{23}	– 20.3 dB	– 37.2 dB
S_{41}	– 23.9 dB	– 34.0 dB
S_{43}	– 19.6 dB	– 24.4 dB

Note: S_{11}, S_{33}: ^{23}Na reflection loss, S_{22}, S_{44}: ^{1}H reflection loss, S_{31}: isolation between channels of ^{23}Na coil, S_{42}: isolation between channels of ^{1}H coil, S_{21}, S_{23}, S_{41}, and S_{43}: isolation amongst channels of both ^{1}H and ^{23}Na coils.

each coil and minimal coupling between the different nuclei.

Figure 2 shows different coronal slices of ^{1}H, ^{23}Na, and ^{23}Na images overlaid on ^{1}H chick embryo MR images, validating the feasibility of using the proposed double-tuned coil for real *in ovo* applications. Despite the chick embryo being only at its developmental day 13, various anatomical structures and body parts are discernible in Figure 2 using both ^{1}H and ^{23}Na MRI. These include a clear outline of the embryo; the eyes indicated by red arrows; the brain highlighted with yellow arrows; the spine pointed out using orange arrows; the allantoic cavity specified by white arrows, with the CAM facing towards the eggshell; and the yolk marked by green arrows. In the sodium images, high sodium levels are evident in the allantoic sac adjacent to the embryo, which functions as an excretory organ. Both the allantoic cavity and the CAM facing the eggshell exhibit high sodium signals due to the active transport of sodium and chloride during embryonic development.[34,35] Furthermore, the eyes of the chick embryo show elevated sodium concentrations, making them distinguishable in the ^{23}Na MR images.

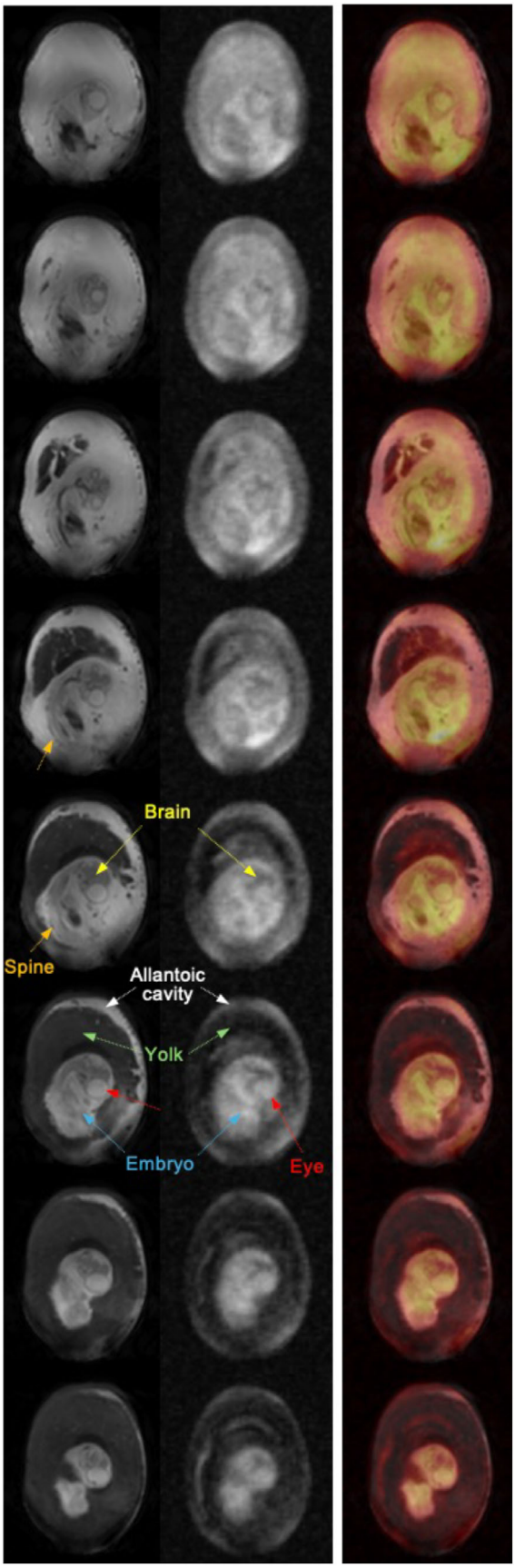

FIGURE 2 ^{1}H, ^{23}Na, and $^{1}H/^{23}Na$ overlaid MR images of 13-day-old chick embryo shown at different coronal slices.

4 | DISCUSSION

The design concept of the proposed double-tuned coil for *in ovo* ^{1}H and ^{23}Na MR was successfully demonstrated both on the bench and on a 7 T MRI scanner. During the design stage, our primary focus was to improve the quality of the ^{23}Na coil to match its single-tuned counterpart, before integrating several possible ^{1}H coil designs into the ^{23}Na coil.

Our initial attempt at designing the double-tuned coil was to use an alternating ^{1}H and ^{23}Na coil arrangement with a 22.5° rotated straight traditional ^{1}H birdcage combined with a recently introduced tapered ^{23}Na coil.

Previous studies[30,31] indicated this approach, but rotating the coil by 22.5° in the axial plane did not work for our setup and we encountered interference issues. Despite taking measures to prevent interference by separating the end-rings of both coils using the tapered design, we were not able to circumvent the problem. While bench tests showed no coupling issues between the channels of the ^{1}H and ^{23}Na coils, when carrying out imaging experiments, the proton images were marred by artfacts and the quality was significantly degraded due to interaction with the ^{23}Na coil.

Incorporating ordinary ^{1}H-blocking traps on the ^{23}Na coil improved the quality of the proton MR images and matched well to those of single-tuned ^{1}H images. However, the insertion of lossy traps in each rung of the ^{23}Na coil unfortunately degraded its quality. As shown in Figure 2, a spiral arrangement minimized interference from the ^{23}Na coil, resulting in improved ^{1}H images without artfacts. The SNR of our ^{23}Na coil remained identical to the single-tuned coil, especially since we avoided the inclusion of lossy components.

To ensure the highest quality of the ^{23}Na coil, we opted against a spiral design for the ^{23}Na coil. This decision was made to avoid the increased conductor length of the coil rungs leading to losses. According to Tomanek et al.,[13] the losses (~35% and ~5% B_1 efficiency losses in a human-sized coil at 81 MHz, similar to our ^{23}Na frequency and at 200 MHz, respectively) become more pronounced at lower frequencies, and the effect of spiring it at the ^{1}H frequency was acceptable. Moreover, animal- or egg-sized coils might not be significantly affected by the extended rung lengths due to their relatively smaller compared to human coils. However, if interference levels become severe, for example, when imaging different objects, a spiral design with a 90° rotation between ^{1}H and ^{23}Na may be an option to help decrease the coupling even further. Furthermore, spiral coil designs could offer extended performance in the z-direction,[12,32] which may be beneficial since the ^{1}H coil was not tapered.[29]

Conducting further optimization, in terms of the end-ring bend shape, spiral angle, coil pattern thickness, or width, may also be useful in improving SNR and/or RF field homogeneity. Moreover, bending the ^{1}H coil towards the end-rings, similar to the tapered ^{23}Na coil, was not pursued due to potential coupling concerns. Other combinations of birdcage coil, for example, high-pass ^{1}H and high-pass ^{23}Na or low-pass ^{1}H and high-pass ^{23}Na were not evaluated.[31] This may leave room for potential improvements, particularly for the ^{23}Na coil.

While our studies were conducted on a clinical scanner, performing these experiments on a small animal scanner[36,37] would be more suitable due to the higher gradient strengths and better resolution capabilities. Improving ^{23}Na image resolution on clinical scanners is limited by a lower gradient strength compared to animal scanners.

Furthermore, this proposed double-tuning technique is not limited to ^{23}Na, and the versatility of our design means it can be adapted for use with other nuclei, such as ^{2}H, ^{13}C, or ^{31}P. This flexibility opens up new avenues for research into energy metabolism, glucose utilization, and other critical biochemical pathways for experimental embryology and teratology. Our coil is not intended for mass production, but rather for use in specific studies focusing on the investigation of, for example, tumor biology or in longitudinal studies.

The use of ^{23}Na MRI provides key physiological and biochemical insights by detecting changes in cellular processes. The improved quality of a double-tuned coil enables precise quantitative analysis and dynamic monitoring of sodium concentrations. Furthermore, auxiliary scans, such as magnetic field mapping and shimming, can be performed using the standard but more sensitive ^{1}H channel without changing the coil. This is particularly important for many advanced ^{23}Na imaging methods, for example, single- and triple-quantum-filtered,[38,39] as they require high demands on magnetic field homogeneity and significantly benefit from precise shimming. This may also enable the imaging of restricted and non-restricted ^{23}Na concentrations in tissues,[39] potentially in conjunction with PET,[40,41] resulting in a versatile imaging apparatus capable of retrieving metabolic, anatomical, and functional imaging information, leveraging the synergistic benefits of three distinct imaging modalities.[42]

5 | CONCLUSIONS

In ovo MR measurements represent a promising approach and an ethical alternative to traditional in vivo preclinical MR experiments using small animals. By utilizing chick embryos, researchers can carry out ethical and expedited examinations using various methodologies while avoiding the complexities and ethical concerns associated with small animal studies. The innovative design of our proposed double-tuned coil, distinguished by its unique arrangement, provides improved performance. Therefore, it has the potential to significantly enhance the quality of *in ovo* ^{1}H and ^{23}Na MRI hybrid measurements. This improved imaging capability may also be crucial for advancing our understanding of developmental biology and for the preclinical testing of new drugs and therapies. In the future, we intend to investigate a wide range of biological and pathological processes using this double-tuned coil, including studying tumor growth, angiogenesis, and response to treatment in the chick embryo model.

ACKNOWLEDGMENTS

The open access publication of this work is funded by the Deutsche Forschungsgemeinschaft (DFG, German Research Foundation) – 491111487. A PhD position for

Sandra Krause was supported by DFG – 513201378. We also thank CR for English proofreading.

CONFLICT OF INTEREST STATEMENT

The authors have no relevant conflicts of interest to disclose.

REFERENCES

1. Hu R, Kleimaier D, Malzacher M, Hoesl MAU, Paschke NK, Schad LR. X-nuclei imaging: current state, technical challenges, and future directions. *J Magn Reson Imaging*. 2020;51(2):355-376. doi:10.1002/jmri.26780
2. Worthoff WA, Shymanskaya A, Choi CH, Felder J, Oros-Peusquens AM, Shah NJ. Multinuclear MR imaging and spectroscopy. *Quantitative MRI of the Brain*. 2nd ed. CRC Press; 2018.
3. Shah NJ, Worthoff WA, Langen KJ. Imaging of sodium in the brain: a brief review. *NMR Biomed*. 2016;29(2):162-174. doi:10.1002/nbm.3389
4. Thulborn K, Lui E, Guntin J, et al. Quantitative sodium MRI of the human brain at 9.4 T provides assessment of tissue sodium concentration and cell volume fraction during normal aging. *NMR Biomed*. 2016;29(2):137-143. doi:10.1002/nbm.3312
5. Thulborn KR, Davis D, Adams H, Gindin T, Zhou J>. Quantitative tissue sodium concentration mapping of the growth of focal cerebral tumors with sodium magnetic resonance imaging. *Magn Reson Med*. 1999;41(2):351-359. doi:10.1002/(SICI)1522-2594(199902)41:2⟨351::AID-MRM20⟩3.0.CO;2-H
6. Ouwerkerk R, Bleich KB, Gillen JS, Pomper MG, Bottomley PA. Tissue sodium concentration in human brain tumors as measured with 23Na MR imaging. *Radiology*. 2003;227(2):529-537. doi:10.1148/radiol.2272020483
7. Inglese M, Madelin G, Oesingmann N, et al. Brain tissue sodium concentration in multiple sclerosis: a sodium imaging study at 3 tesla. *Brain*. 2010;133(3):847-857. doi:10.1093/brain/awp334
8. Konstandin S, Nagel AM. Measurement techniques for magnetic resonance imaging of fast relaxing nuclei. *Magn Reson Mater Phy*. 2014;27(1):5-19. doi:10.1007/s10334-013-0394-3
9. Choi CH, Hong SM, Felder J, Shah NJ. The state-of-the-art and emerging design approaches of double-tuned RF coils for X-nuclei, brain MR imaging and spectroscopy: a review. *Magn Reson Imaging*. 2020;72:103-116. doi:10.1016/j.mri.2020.07.003
10. Matson GB, Vermathen P, Hill TC. A practical double-tuned 1H/31P quadrature birdcage headcoil optimized for 31P operation. *Magn Reson Med*. 1999;42(1):173-182. doi:10.1002/(sici)1522-2594(199907)42:1⟨173::aid-mrm23⟩3.0.co;2-o
11. Fitzsimmons JR, Beck BL, Ralph Brooker H. Double resonant quadrature birdcage. *Magn Reson Med*. 1993;30(1):107-114. doi:10.1002/mrm.1910300116
12. Alsop DC, Connick TJ, Mizsei G. A spiral volume coil for improved RF field homogeneity at high static magnetic field strength. *Magn Reson Med*. 1998;40(1):49-54. doi:10.1002/mrm.1910400107
13. Tomanek B, Volotovskyy V, Gruwel MLH, McKenzie E, King SB. Double-frequency birdcage volume coils for 4.7T and 7T. *Concepts Magn Reson B: Magn Reson Eng*. 2005;26B(1):16-22. doi:10.1002/cmr.b.20038
14. Murphyboesch J, Srinivasan R, Carvajal L, Brown TR. Two configurations of the four-ring birdcage coil for 1H imaging and 1H-decoupled 31P spectroscopy of the human head. *J Magn Reson, Series B*. 1994;103(2):103-114. doi:10.1006/jmrb.1994.1017
15. Rath AR. Design and performance of a double-tuned bird-cage coil. *J Magn Reson (1969)*. 1990;86(3):488-495. doi:10.1016/0022-2364(90)90026-6
16. Hancu I, Boada FE, Shen GX. Three-dimensional triple-quantum-filtered23Na imaging of in vivo human brain. *Magn Reson Med*. 1999;42(6):1146-1154. doi:10.1002/(SICI)1522-2594(199912)42:6⟨1146::AID-MRM20⟩3.0.CO;2-S
17. Lim H, Thind K, Martinez-Santiesteban FM, Scholl TJ. Construction and evaluation of a switch-tuned (13) C—(1) H birdcage radiofrequency coil for imaging the metabolism of hyperpolarized (13) C-enriched compounds. *J Magn Reson Imaging*. 2014;40(5):1082-1090. doi:10.1002/jmri.24458
18. Dabirzadeh A, McDougall MP. Trap design for insertable second-nuclei radiofrequency coils for magnetic resonance imaging and spectroscopy. *Concepts Magn Reson B: Magn Reson Eng*. 2009;35B(3):121-132. doi:10.1002/cmr.b.20139
19. Ha Y, Choi CH, Worthoff WA, et al. Design and use of a folded four-ring double-tuned birdcage coil for rat brain sodium imaging at 9.4 T. *J Magn Reson*. 2018;286:110-114. doi:10.1016/j.jmr.2017.12.003
20. Wiggins GC, Brown R, Lakshmanan K. High-performance radiofrequency coils for 23Na MRI: brain and musculoskeletal applications. *NMR Biomed*. 2016;29(2):96-106. doi:10.1002/nbm.3379
21. Shajan G, Mirkes C, Buckenmaier K, Hoffmann J, Pohmann R, Scheffler K. Three-layered radio frequency coil arrangement for sodium MRI of the human brain at 9.4 Tesla. *Magn Reson Med*. 2016;75(2):906-916. doi:10.1002/mrm.25666
22. Hong SM, Choi CH, Shah NJ, Felder J. Design of a folded, double-tuned loop coil for ^{1}H/X-nuclei MRI applications. *IEEE Trans Med Imaging*. 2023;42(5):1424-1430. doi:10.1109/TMI.2022.3228305
23. Meyerspeer M, Serés Roig E, Gruetter R, Magill AW. An improved trap design for decoupling multinuclear RF coils. *Magn Reson Med*. 2014;72(2):584-590. doi:10.1002/mrm.24931
24. Ha Y, Choi CH, Shah NJ. Development and implementation of a PIN-diode controlled, quadrature-enhanced, double-tuned RF coil for sodium MRI. *IEEE Trans Med Imaging*. 2018;37(7):1626-1631. doi:10.1109/TMI.2017.2786466
25. Choi CH, Hong SM, Ha Y, Shah NJ. Design and construction of a novel 1H/19F double-tuned coil system using PIN-diode switches at 9.4T. *J Magn Reson*. 2017;279:11-15. doi:10.1016/j.jmr.2017.04.005
26. Brown R, Lakshmanan K, Madelin G, et al. A flexible nested sodium and proton coil array with wideband matching for knee cartilage MRI at 3T. *Magn Reson Med*. 2016;76(4):1325-1334. doi:10.1002/mrm.26017
27. Herrmann A, Taylor A, Murray P, Poptani H, Sée V. Magnetic resonance imaging for characterization of a chick embryo model of cancer cell metastases. *Mol Imaging*. 2018;17:1536012118809585. doi:10.1177/1536012118809585
28. Miebach L, Berner J, Bekeschus S. In ovo model in cancer research and tumor immunology. *Front Immunol*. 2022;13:1006064. doi:10.3389/fimmu.2022.1006064
29. Choi CH, Bruch M, Hong SM, et al. A modified quadrature birdcage coil incorporated with a curved feature for in ovo MRI at 7 T. *IEEE OJEMB*. 2024;5:534-541. doi:10.1109/OJEMB.2024.3420231
30. Fantasia M, Galante A, Maggiorelli F, et al. Numerical and workbench design of 2.35 T double-tuned (^{1}H/^{23}Na) nested RF birdcage coils suitable for animal size MRI. *IEEE Trans Med Imaging*. 2020;39(10):3175-3186. doi:10.1109/TMI.2020.2988599
31. Zhang B, Lowrance D, Sarma MK, et al. 3T 31P/1H calf muscle coil for 1H and 31P MRI/MRS integrated with NIRS data acquisition. *Magn Reson Med*. 2024;91(6):2638-2651. doi:10.1002/mrm.30025
32. Pak JS, Kim J, Lee JO, et al. A new 3.0T hybrid-spiral-birdcage (HSB) coil for improved homogeneity along Z-axis. *Proc Intl Soc Mag Reson Med*. 2000:1393.
33. Yushkevich PA, Piven J, Hazlett HC, et al. User-guided 3D active contour segmentation of anatomical structures: significantly improved efficiency and reliability. *Neuroimage*. 2006;31(3):1116-1128. doi:10.1016/j.neuroimage.2006.01.015
34. Gabrielli MG, Accili D. The chick chorioallantoic membrane: a model of molecular, structural, and functional adaptation

to transepithelial ion transport and barrier function during embryonic development. *J Biomed Biotechnol*. 2010;2010:940741.
35. Kundeková B, Máčajová M, Meta M, Čavarga I, Bilčík B. Chorioallantoic membrane models of various avian species: differences and applications. *Biology*. 2021;10(4):301.
36. Choi CH, Ha Y, Veeraiah P, Felder J, Möllenhoff K, Shah NJ. Design and implementation of a simple multinuclear MRI system for ultra high-field imaging of animals. *J Magn Reson*. 2016;273:28-32. doi:10.1016/j.jmr.2016.10.007
37. Felder J, Celik AA, Choi CH, Schwan S, Shah NJ. 9.4 T small animal MRI using clinical components for direct translational studies. *J Transl Med*. 2017;15(1):264. doi:10.1186/s12967-017-1373-7
38. Fiege DP, Romanzetti S, Mirkes CC, Brenner D, Shah NJ. Simultaneous single-quantum and triple-quantum-filtered MRI of 23Na (SISTINA). *Magn Reson Med*. 2013;69(6):1691-1696. doi:10.1002/mrm.24417
39. Worthoff WA, Shymanskaya A, Shah NJ. Relaxometry and quantification in simultaneously acquired single and triple quantum filtered sodium MRI. *Magn Reson Med*. 2019;81(1):303-315. doi:10.1002/mrm.27387
40. Worthoff WA, Shymanskaya A, Lindemeyer J, Langen KJ, Shah NJ. Relaxometry and quantification in sodium MRI of cerebral gliomas: a FET-PET and MRI small-scale study. *NMR Biomed*. 2020;33(10):e4361. doi:10.1002/nbm.4361
41. Choi CH, Stegmayr C, Shymanskaya A, et al. An in vivo multimodal feasibility study in a rat brain tumour model using flexible multinuclear MR and PET systems. *EJNMMI Phys*. 2020;7(1):50. doi:10.1186/s40658-020-00319-6
42. Shah NJ. Multimodal neuroimaging in humans at 9.4 T: a technological breakthrough towards an advanced metabolic imaging scanner. *Brain Struct Funct*. 2015;220(4):1867-1884. doi:10.1007/s00429-014-0843-4

How to cite this article: Choi C-H, Hong S-M, Felder J, et al. Design, construction, and use of a tapered-spiral, quadrature $^{1}H/^{23}Na$ double-tuned coil for *in ovo* MRI at 7 T. *Med Phys*. 2024;51:8761–8767.
https://doi.org/10.1002/mp.17448